Bloch simulations with intra-voxel spin dephasing

Latta, Peter; Gruwel, Marco L. H.; Jellus, Vladimir; Tomanek, Boguslaw

National Research Council Canada   Conseil national de recherches Canada

Canada

Bloch simulations with intra-voxel spin dephasing

Peter Latta[1,2], Marco L. H. Gruwel[1], Vladimír Jellúš[3], Boguslaw Tomanek[1]

[1]Institute for Biodiagnostics
National Research Council of Canada
435 Ellice Avenue
Winnipeg
Manitoba, Canada. R3B 1Y6

[2]Institute of Measurement Science
Slovak Academy of Sciences
Dúbravská cesta 9
SK-84219 Bratislava, Slovakia

[3]Imaging & IT Division
Magnetic Resonance
H IM MR PLM AW Orthopedics
Siemens AG
Allee am Roethelheimpark 2
91052 Erlangen, Germany

Address for Correspondence:
Peter Latta
Institute for Biodiagnostics
435 Ellice Avenue
Winnipeg
Manitoba
Canada. R3B 1Y6
Tel: (204) 984 4544
Fax: (204) 984 7036
E-mail: peter.latta@nrc-cnrc.gc.ca

Running Title: Bloch simulations with intra-voxel spin dephasing

Submitted as a research article to Journal of Magnetic Resonance

Abstract.

A common problem in simulations of MRI-experiments based on the numerical solution of the Bloch equations is the finite number of isochromats used in the calculations. This usually results in false or spurious signals and is a source of various differences between calculated and experimentally obtained data. In this paper, we are proposing a technique representing each sample voxel by a central and three additional isochromats, slightly shifted in orthogonal directions from center, thus providing a linear approximation of intravoxel dephasing. This approach allows for further improvement and precision of the calculated NMR signal and virtually avoids the problem related to an finite set of isochromats. Here we provide details of the algorithm together with examples of simulations which prove the efficiency of this approach.

1. Introduction

There are numerous situations where computer simulations have become a useful tool for studying various aspects of MR experiments, pulse sequences and hardware configurations. One of the most common and flexible categories of such simulators is based on the discrete-iterative solution of the Bloch equations applied to the spin system [1]. This method allows one, in a simple and convenient way, to investigate most phenomena occurring during magnetic resonance imaging (MRI) experiments. However, despite the flexibility of such models, the common problem with this approach is the finite set of isochromats used in the calculation. This affects formation of the output data in the following ways:

- the accuracy of the calculated signal from each volume element depends on the number of isochromats used per spatial dimension in the simulation,

- simulated data generally have a discrete frequency spectrum as the limited set of spins used in these calculation only contributes a certain number of frequencies to the signal,

- the discrete and regular location of the spins in simulations can generate false signals caused by rephasing of the transverse magnetization, e.g. by applying strong spoiler gradients.

A number of different approaches to deal with this problem have been suggested in the past. One possible way is to use multiple isochromats in each volume element, which helps to obtain a more realistic signal and, to some extend, the suppression of spurious signal. It has been shown that to achieve an image reconstruction error below 1.5% at least three

isochromats per voxel and spatial direction have to be used [2] . However, even with multiple spins per voxel, spurious signal could appear if the gradient amplitude/duration exceeds certain limits. Therefore, the spin density distribution and/or appropriate isochromat spacing has to be considered prior to simulation experiments [3][4]. The randomization of spin-spin distances within the voxel could be used to suppress spurious rephasing as well [5], however, this method induces additional stochastic noise into the simulated data [6].

As the intra-voxel dephasing (IVD) from main field inhomogeneities ΔB_0, and imaging gradients strongly affects MRI signal formation, the incorporation of this phenomenon would provide a more realistic simulation. In [7], the additional T_2^* exponential weighting of signal has been applied in order to reflect dephasing from ΔB_0 inhomogeneities. However, this approach requires special treatment of the time scale in order to generate proper spin-echo signal formation by 180^0 refocusing pulses. Another approach assumes a linear phase change across the voxel which determines the dephasing slope for the phase of the neighboring isochromats, and finally, integration of transverse magnetization is used to calculate the signal generated by each element [8]. An alternative approach is to calculate intra-voxel dephasing iteratively using an analytical formula for partial derivatives of the magnetization vectors [9].

In this work we are proposing a simple alternative approach to estimate the intra-voxel dephasing in Bloch simulators from the mutual phase difference of closely placed pairs of isochromats [10]. The technique is relatively computational efficient as it requires usage of only one extra isochromat for each spatial dimension considered in the simulation, and at the

4

same time is resistive to the generation of spurious echoes as the spacing of spins can be chosen to be very small.

2. Methods

2.1 Spin modeling

The typical approach exploited in most Bloch simulators includes the following steps:

• Construction of the discrete virtual object – a 1D, 2D or 3D matrix, where each element holds information about a local physical property such as: spin density, relaxation constants T_1 and T_2, ΔB_0 field inhomogeneity etc. Each voxel contains one or more magnetization vectors as well. The matrix represents a real object, which is assumed to consist of rectangular, homogeneous and homogeneously excited voxels. It is the goal of the approach presented in the paper to improve the accuracy of the representation of the rectangular voxel volume, which would normally be absent in the pointwise representation.

• Numerical solution of the Bloch equation is applied for each element of the virtual object. Calculations are performed step by step following the evolution of experimental parameters such as the radiofrequency field (RF) $B_1(r,t)$, the gradient field $G(t)$, and in some cases dynamic properties e.g. flow [11]. The evolution of the magnetization vector $M(r,t) = (M_x, M_y, M_z)^T$ in the rotating laboratory frame can be calculated from time instance t_i to t_{i+1} as:

$$M(r,t_{i+1}) = E\, R_{Rot}\left(B_1(r,t_i), \left(0,0,G(t_i)\cdot r\right)^T, \Delta B_0(r)\right) M(r,t_i) + E_0 \quad (1)$$

5

where R_{Rot} is a rotation operator which can be found in the literature e.g. [1][9][12]. The diagonal matrix $E{=}diag\left(e^{-\Delta t/T_2}, e^{-\Delta t/T_2}, e^{-\Delta t/T_1}\right)$ and the column vector $E_0 = \left(0, 0, M_0\left(1-e^{-\Delta t/T_1}\right)\right)^T$ introduce the relaxation and M_0 represents the initial magnetization in the equilibrium state.

- The NMR signal of the sample, acquired at time instance t_i, is calculated by summation of the transverse components of magnetization vector over the all elements in the virtual object:

$$s(t_i) = \sum_r \left(M_x(r,t_i) + j\, M_y(r,t_i)\right) \tag{2}$$

where $j = \sqrt{-1}$.

2.2 Tracking of intra-voxel dephasing

Although calculation of the output signal using Eq.(2) is simple and straightforward in certain situations, output data are substantially different from results obtained in real NMR experiments. Perhaps the most obvious difference is related to the rephasing of false transverse magnetization as a consequence of insufficient isochromat spacing used in the simulation. When the model only contains a single isochromat per voxel, the mutual phase difference between neighboring isochromats in a given spatial dimension is:

$$\vartheta_n = \pm\left|k_n\right|\,\Delta r_n \qquad n = x,\, y,\, z \tag{3}$$

where $|k_n|$ is distance of the $\boldsymbol{k}$-space trajectory from the origin and Δr_n represents the isochromat spacing. The phase difference ϑ_n is repeating with cycle of $2\pi/{\Delta r_n}$, which determines the replication or modulation of the signal in k-space, calculated according to Eqn.(2). The desired image resolution dictates that signal is sampled over the $\boldsymbol{k}$-space span $k_n = 2\pi/{w_n}$, where w_n is the image voxel size. In order to avoid image artifacts related to signal replication in $\boldsymbol{k}$-space, the following condition has to be fulfilled:

$$w_n \geq \Delta r_n \tag{4}$$

Incorporation of IVD into signal calculations could significantly suppress problems with rephasing of transverse magnetization and at the same time improve the precision of signal estimation. However, in order to do so it is imperative to track exact IVD in time during the evolution of isochromats. Here we are suggesting a simple solution for IVD monitoring, which could be used as an alternative to the analytically based method. The idea is to utilize extra isochromats, one per used spatial dimension, and to position them very close to the central isochromat as is shown in Fig.1. Assuming a linear approximation of the phase-change within the voxel, dephasing in each direction is then calculated as the phase difference between the central and the corresponding off-center isochromat divided by their mutual distance:

$$\varphi_n' = \frac{\varphi_n - \varphi_c}{h}, \qquad \text{n = x,y,z} \tag{5}$$

where φ_n' represents a phase gradient, φ_c the central isochromat's phase, φ_n the off-center isochromat's phase in the corresponding spatial dimension and h the distance between the

central and the off-center spins. The signal from the voxel affected by IVD can thus be calculated by integration of the phase over the whole voxel volume [8][9][13]:

$$s(\mathbf{r},t_i) = \int\limits_{-\frac{\Delta r_x}{2}}^{\frac{\Delta r_x}{2}} \int\limits_{-\frac{\Delta r_y}{2}}^{\frac{\Delta r_y}{2}} \int\limits_{-\frac{\Delta r_z}{2}}^{\frac{\Delta r_z}{2}} \left| M_{XY}(\mathbf{r},t_i) \right| e^{i(\varphi'_x(\mathbf{r},t_i)x + \varphi'_y(\mathbf{r},t_i)y + \varphi'_z(\mathbf{r},t_i)z + \varphi_c(\mathbf{r},t_i))} \, dx\,dy\,dz$$

$$= \left| M_{XY}(\mathbf{r},t_i) \right| e^{i\varphi_c(\mathbf{r},t_i)} sinc\left(\tfrac{\Delta r}{2}\varphi'_x(\mathbf{r},t_i)\right) sinc\left(\tfrac{\Delta r}{2}\varphi'_y(\mathbf{r},t_i)\right) sinc\left(\tfrac{\Delta r}{2}\varphi'_z(\mathbf{r},t_i)\right)$$

(6)

Where the sinc function takes the un-normalized form of $sin(x) / x$. As the three off-center isochromats serve the purpose to monitor phase evolution only, their distance from the center isochromat can be very small, and is in practice only limited by computational accuracy of the computer's double precision arithmetic. The close isochromat spacing helps to keep the isochromat's phase difference within the $\pm\pi$ range and makes the tracking of IVD possible, even when very long gradient pulses or large ΔB_0 field inhomogeneities are applied. All simulations presented in this paper used the same off-center isochromat distance of $h=10^{-9}$ m.

3. Simulation results and discussion

The proposed IVD algorithm was implemented on a homemade stand-alone Bloch simulator written in C/C++ in a Unix environment. All simulations were prepared by Matlab version 7.4 (The MathWorks, Natick, MA, USA) program scripts, which generated the input data such as the phantoms, the inhomogeneity maps, and the pulse sequences. These were sent to the simulator for execution. After the simulation was finished, the Matlab script read and processed the output data from the simulator and displayed the results on the screen. The Matlab script measured the simulation time from start to finish of the Bloch simulator run, i.e. the overhead including preparing and processing the data was not included. All simulations were performed on a 2.5 GHz dual core CPU laptop computer running Windows/XP. The Cygwin emulator of the Unix operating system was used to run the Bloch simulator in the Windows/XP.

In the following, the input matrix size will refer to the dimensions of the phantom voxel arrays used by the Bloch simulator to generate NMR signal. The output matrix size will refer to the dimensions of the sampled NMR signal i.e. the k-space matrix and/or reconstructed image.

3.1 FID simulations

Figure 2 compares analytical and simulated magnitudes of the FID signal from a 1D boxcar object of 0.5 mm length with a 36 mT/m applied gradient field. The analytical signal was calculated using equation (6) applied for a 1D object. In the simulation, only one voxel was

used containing a central and three off-center isochromats, however, two of them had no effect on the signal formation as their shifts were perpendicular to the applied gradient. Both data sets demonstrate excellent agreement between theoretical and simulated signal.

3.2 Voxel spectrum simulations

Frequency spectra from a 1D boxcar object were collected in two different ways. The first calculation used a single center and three offset isochromats, and included the IVD technique. The second calculation was performed on 1000 uniformly distributed isochromats within the boxcar object of identical size. The results of these calulations are shown in Fig. 3. The parameters used in both simulations are as follows: gradient echo sequence with a 50 μs hard pulse excitation, object size is 0.5 mm (1 voxel), gradient amplitude 63 mT/m, sampling frequency 10 kHz and 1000 complex points acquisition. The spectra are almost identical, with a frequency bandwidth of 1340.5 Hz in case of IVD and 1342.8 Hz for the multiple isochromats simulation, both measured as full width at half maximum (FWHM) intensity. This is very close to a bandwidth of 1343.586 Hz calculated from the gradient amplitude and voxel size. IVD generates a uniform spectral distribution with a frequency bandwidth modulated by the applied gradient field along the corresponding direction.

In addition, IVD makes it possible to use a significantly smaller number of isochromats, what is demonstrated on phantom which contains four vertical strips of relative width 1,2,3 and 4 (see Fig.4). The image (A) was generated from the phantom of 256x256 input matrix size and without usage of IVD algorithm. In the simulation of image (B), the phantom of 16x16-matrix size with combination of IVD algorithm has been used. Both output images have the same resolution of 256x256 pixels and appear almost identical, though a closer look

at the profile of image (B) reveals ringing artifact at the edges of the high-low intensities transitions. However, there was a significant (approximately 78 times) reduction in the simulation time needed to generate image (B) due the smaller number of isochromats used in the calculation.   The ripple artifact in IVD simulations could be suppressed choosing a higher phantom resolution as demonstrated in image (C). The image (C) used the same input and output matrix size of 256x256 voxels, however, for image (C) the computational time was approximately 200 longer. The simulation parameters for image (D) were identical to those for experiment (B), with the exception of the IVD application. The obtained image (D) reveals that the frequency lines from the neighboring isochromats are separated from each other. The simulation demonstrates it fails to meet requirements on resolution of the phantom model and the image i.e. condition given by Eqn. (4). The previous examples demonstrate how IVD modifies the voxel spectrum character, which now reminds the user more of a spectrum obtained from the continuous spin distribution rather than from the discrete isochromat grid. This permits us to speed up the simulations using isochromat matrices with a significantly smaller size as the simulated image resolution and, at the same time, it avoids any severe spectral distortions.

3.3 Spurious signal suppression

Fig. 5 shows an example of the gradient-echo (A) and spin-echo (D) pulse sequence. Simulation parameters were as follows: 1D phantom with a matrix size of 128 voxels, FOV = 50 mm, gradient amplitude 20 mT/m, echo time 12 ms and 10 µs time steps. The results obtained without considering IVD contain three additional spurious echoes shown in

(B) and (E). These false signals can be effectively suppressed using IVD, as is shown in (C) and (F).

3.4 Echo train simulations

Two echo train examples are presented: a multiple spin-echo i.e., Carr-Purcell-Meiboom-Gill (CPMG) and a multiple gradient pulse sequence (see Fig.6). In both simulations, an input phantom with the following parameters has been used: single voxel with a size of 5 mm in each dimension, $T_1 = 600$ms and $T_2 = 200$ms. The IVD technique modulated the echo formation from the single voxel using a 0.5 mT/m linear field inhomogeneity applied across the voxel in each dimension. Note that the apparent T_2^* modulation of the echo amplitude in the multi gradient echo experiment represents a modulation due to both IVD as well as a T_2 relaxation effect.

3.5 Truncation artifact

When applying IVD in Bloch simulations, it introduces a ringing or so-called Gibbs artifact into the output images. This is especially well visible when simulations are using lower output image resolution. It might be considered a disadvantage using the IVD algorithm and introducing such artifacts into the reconstructed data. However, when comparing simulated with experimentally obtained data, similar artifacts can be found there as well, as demonstrated in Fig.7. Both experimental (A) and IVD simulated images (B) contain Gibbs artifacts, which tend to be much less visible in higher resolution datasets. It should be noted that these artifacts are not visible in simulations with a single isochromat per voxel as is demonstrated by images in the bottom row (C). The behavior and source of the Gibbs artifact

is similar for both the experimental results and the data simulated with IVD. The artifacts are more pronounced when abrupt intensity changes are presented in the object and for data sets with low *k*-space coverage [14]. We do not see the Gibbs artifact in simulated images as a disadvantage of the IVD method but as a specific feature of the model, able to reproduce experimental performance limitations and imperfections.

3.6 Inhomogeneity induced signal decay.

In order to verify the effect of susceptibility on the simulation, we compare simulated and experimentally obtained data from a 3T spectrometer using a cylindrical phantom containing an axially placed air-filled tube. The phantom was positioned with its long axis perpendicular to the static magnetic field $\mathbf{B_0}$. The field inhomogeneity through the phantom was calculated using a formula for the phantom containing a glass tube (i.d. = 18.8 mm, o.d. = 22.8 mm) according to [15]. The Bloch simulator used this field map to interpolate the inhomogeneity induced by the gradients through the voxel [8]. The following parameters were used in both simulations and experiments: gradient echo sequence with FOV = 120 mm, 128x128-matrix size, TE = 10, 15 and 25 ms, TR = 1000 ms, 90 Hz bandwidth per pixel. The sample relaxation times were estimated to be T_1= 1200 ms and T_2 = 800 ms. Figure 8 illustrates the impact of field inhomogeneities on the output images with increasing echo time. From the experimentally obtained images it is obvious that the area of pixel intensity decay around the air-filled tube is increasing with the usage of longer echo times. The intensity profiles through the phantom center demonstrate that simulated data obtained with IVD exhibit very good agreement with experiment. It should be noted that, using only a single isochromat per voxel without any account for IVD, the model is not capable to realistically simulate the effect of field perturbations and the results substantially deviate from the experimentally

13

obtained data. In [9] it was estimated that in order to obtain reasonable simulation results, at least 8 isochromats per directions are necessary when the multiple isochromats summation strategy is used. The previous results indicate that usage of the IVD algorithm could be much more computationally efficient for the tracking of susceptibility-induced intravoxel dephasing compared to the summation of transverse magnetization from multiple voxels.

The presented IVD algorithm is assuming a linear approximation of the phase change over the voxel. As it was shown in previous examples, for many situations this simplification is reasonable and the linear phase approximations leads to good results. However, when multiple selective excitations are used, the phase change can substantially deviate from the linear assumption. In such cases, the applicability of the method and/or special care for simulation parameters such as spatial discretization of the sample has to be considered prior to the simulations.

4. Conclusion

The proposed intra-voxel dephasing method provides a simple and efficient way to accurately simulate MR signal attenuation for different experimental settings. The algorithm is based on the calculation of differences in transverse orientations for spin pairs in close proximity. Our simulation examples showed good agreement with experimentally obtained data sets. The main characteristics and benefits of the proposed method can be summarized as follows:

- simple and straightforward implementation of IVD algorithm,

- it helps to suppress problems commonly encountered in simulations using a limited number of isochromats, such as spurious echoes and truncation artifacts,

- the spectral features of the signal generated with IVD resemble that of a real sample with a large number of spins.

- the simulated data show a similar k-space span coverage behavior as is typical in real experiments i.e. reconstructed images exhibit Gibbs artifacts and imperfections for which signal intensities depend on the matrix size,

- it required only one extra isochromat for each considered dimension, which makes the simulation relatively time efficient,

- it is applicable to the simulation of the effects of RF pulses and gradient trains on the magnetization,

- it is capable to correctly and efficiently simulate the effect of susceptibility induced field perturbations on experimentally obtained images.

References

[1]   J.Bittoun, J.Taquin, M.Sauzade,   A computer algorithm for the simulation of any nuclear magnetic resonance (NMR) imaging method, *Magn Reson Imaging*, **2** (1984) pp. 113-120.

[2]   P.Shkarin, R.Spencer,   Time domain simulation of Fourier imaging by summation of isochromats, *International Journal of Imaging Systems and Technology*, **8** (1997) pp. 419-426.

[3]   P.Shkarin, R.Spencer,   Direct simulation of spin echoes by summation of isochromats , *Concepts in Magnetic Resonance Part A*, **8** (1996) pp. 253-268.

[4]   R.K.Kwan, A.C.Evans, G.B.Pike,   MRI simulation-based evaluation of image-processing and classification methods, *IEEE Trans Med Imaging*, **18** (1999) pp. 1085-1097.

[5]   R.M.Summers, L.Axel, S.Israel,   A computer simulation of nuclear magnetic resonance imaging, *Magn Reson Med*, **3** (1986) pp. 363-376.

[6]   J.Sharp, D.Yin, R.Tyson, K.Lo, B.Tomanek,   An Integrated MR Console / MR Physics Simulation System, ISMRM 14th Scientific meeting, Seattle, 2006, p.1351

[7]   H.Benoit-Cattin, G.Collewet, B.Belaroussi, H.Saint-Jalmes, C.Odet, The SIMRI project: a versatile and interactive MRI simulator, *J Magn Reson*, **173** (2005) pp. 97-115.

[8]   D.A.Yoder, Y.Zhao, C.B.Paschal, J.M.Fitzpatrick,   MRI simulator with object-specific field map calculations, *Magn Reson Imaging*, **22** (2004) pp. 315-328.

[9]   T.H.Jochimsen, A.Schäfer, R.Bammer, M.E.Moseley,   Efficient simulation of magnetic resonance imaging with Bloch-Torrey equations using intra-voxel magnetization gradients, *J Magn Reson*, **180** (2006) pp. 29-38.

[10]   P.Latta, M.L.H.Gruwel, V.Jellus, B.Tomanek,   Bloch simulation with intra voxel spin dephasing, 25th Annual Scientific Meeting, Valencia, 2008

[11]   I.Marshall, Simulation of in-plane flow imaging, *Concepts in Magnetic Resonance*, **11** (1999) pp. 379-392.

[12]   Y.A.Tesiram, F.Separovic,   Matrix method for analysis of selective NMR pulses, *Concepts in Magnetic Resonance Part A*, **25A** (2005) pp. 1-17.

[13]   P.Latta, M.L.H.Gruwel, V.Volotovskyy, M.H.Weber, B.Tomanek, Simple phase method for measurement of magnetic field gradient waveforms, *Magn Reson Imaging*, **25** (2007) pp. 1272-1276.

[14]   K.T.Block, M.Uecker, J.Frahm, Suppression of MRI truncation artifacts using total variation constrained data extrapolation, *Int J Biomed Imaging*, (2008) p. 184123.

[15]   F.De Guio, H.Benoit-Cattin, A.Davenel,   Signal decay due to susceptibility-induced intravoxel dephasing on multiple air-filled cylinders: MRI simulations and experiments, *MAGMA*, **21** (2008) pp. 261-271.
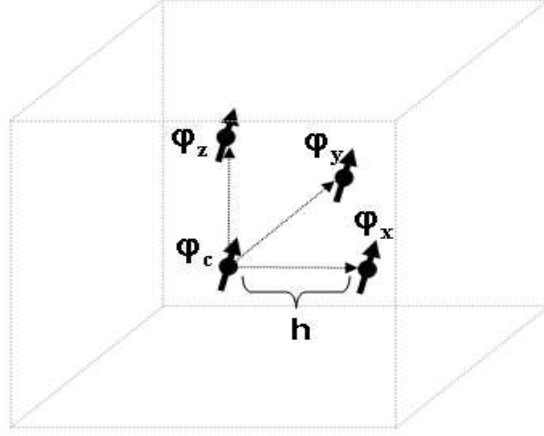
Fig.1 Voxel representation used in the Bloch simulations. Three off-center isochromats are used to monitor the evolution of intra-voxel dephasing. As the mutual distance between central and off-center spins is very small (h $=10^{-9}$ m is used in this paper) the accumulated phase differences can be kept within $\pm\pi$ which makes it easy to calculate intra-voxel dephasing.
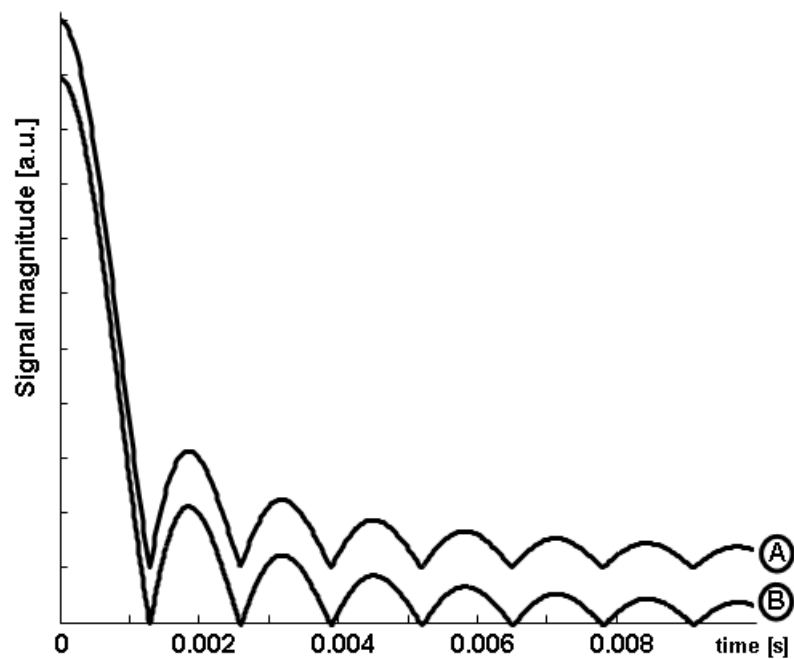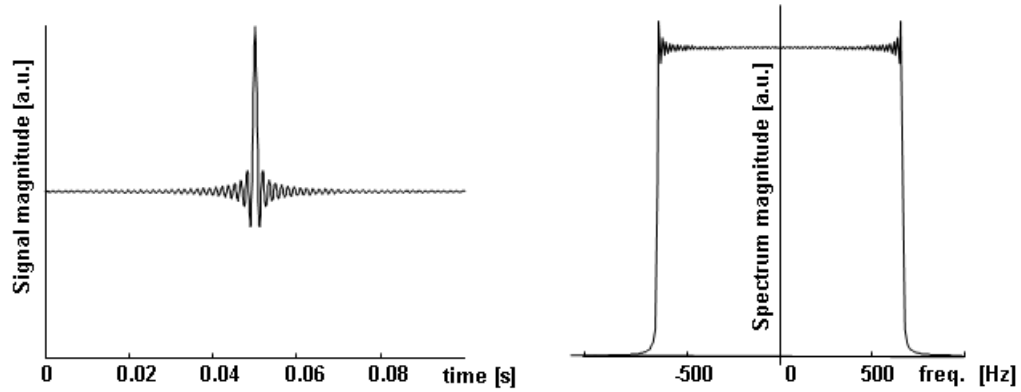
Fig.2 Comparison of FID signals obtained from: (A) analytical equation (signal is shifted up to avoid overlap) and (B) Bloch simulation.

Fig.3 Comparison of the echo signal from a voxel containing a single, central, isochromat using the IVD technique i.e. three off-center additional isochromats (A), versus the signal from 1000 uniformly distributed isochromats (B). The signals are almost identical and have a similar spectral width: 1340.5 Hz in case of IVD and 1342.8 Hz for the 1000 isochromats set.
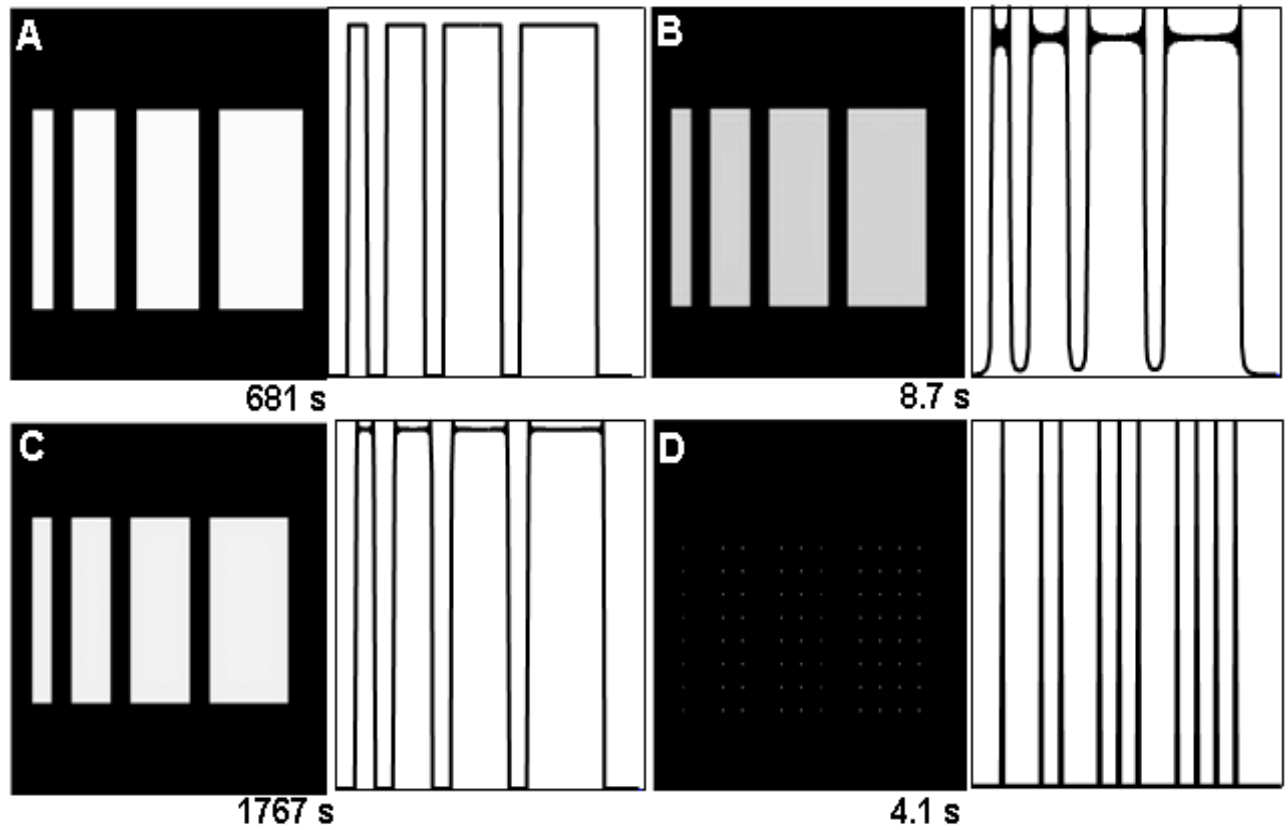
Fig.4 Simulated images obtained from a phantom containing four strips, shown on the left hand side, and the corresponding signal intensity profile, shown on the right hand side. All simulations were performed with the same 256x256-output matrix resolution; however, there was difference in phantom matrix resolution and IVD application: (A) 256x256 without IVD, (B) 16x16 with IVD, (C) 256x256 with IVD and (D) 16x16 without IVD. The output image (D) contains only discrete frequencies corresponding to the position of the isochromats. The time required for simulation is indicated at bottom of each image.
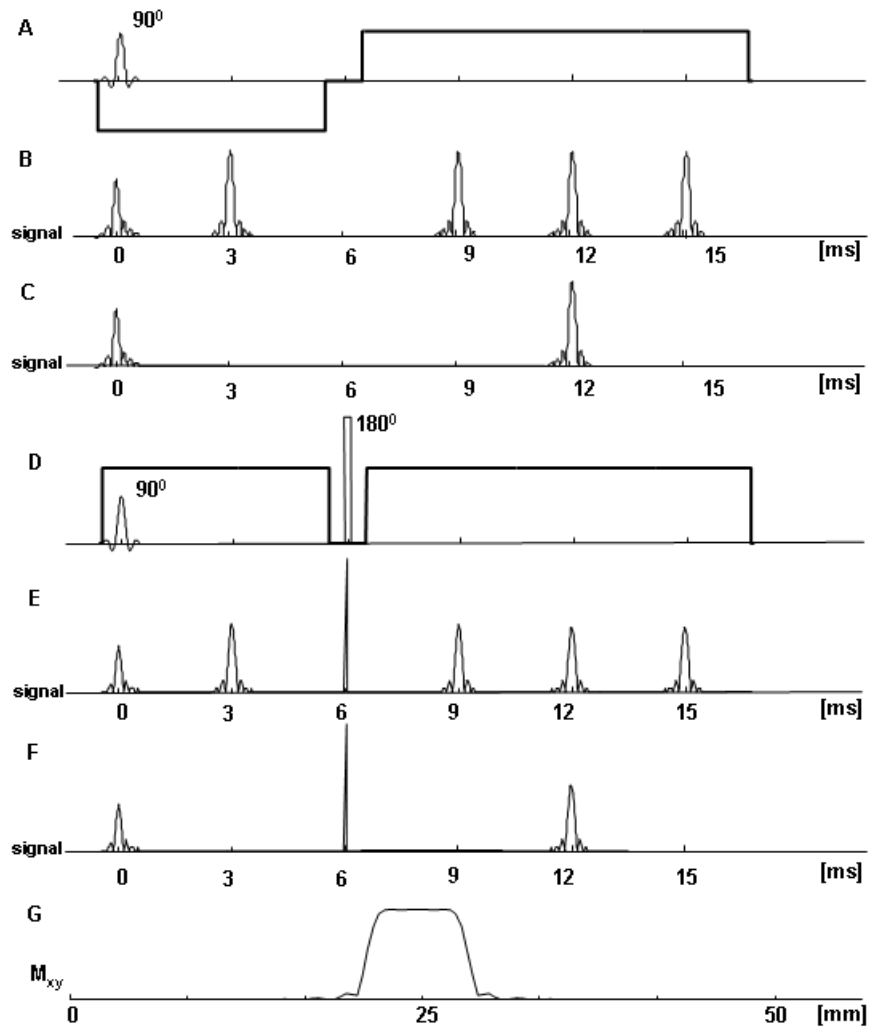
Fig.5 Examples of the gradient echo (A-C) and spin-echo sequences (D-F) and the corresponding excited signals. The signals generated without intra-voxel dephasing exhibits false spurious echoes (B) and (E), which disappear when IVD dephasing is applied (C) and (F). The excitation profile is shown in (G).
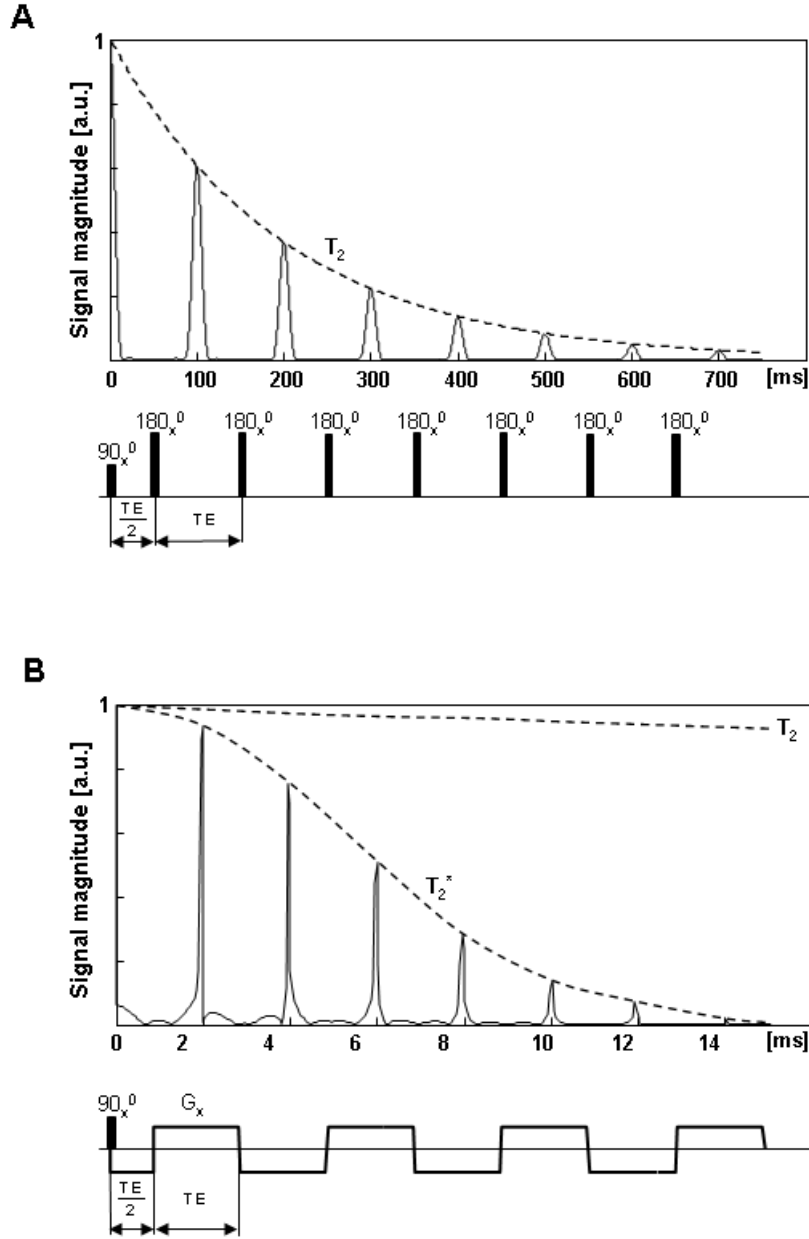
Fig.6 Simulation of the echo trains: (A) CPMG sequence, with echo time 100 ms and (B) the multi-gradient echo sequence, with an echo time of 2ms and a alternating 100 mT/m gradient pulse. In the simulations, the echo formation and T_2^* decay is generated by a single voxel using the IVD technique (four isochromats in total) combined with a 0.5 mT/m linear field inhomogeneity applied across the voxel in each spatial direction.
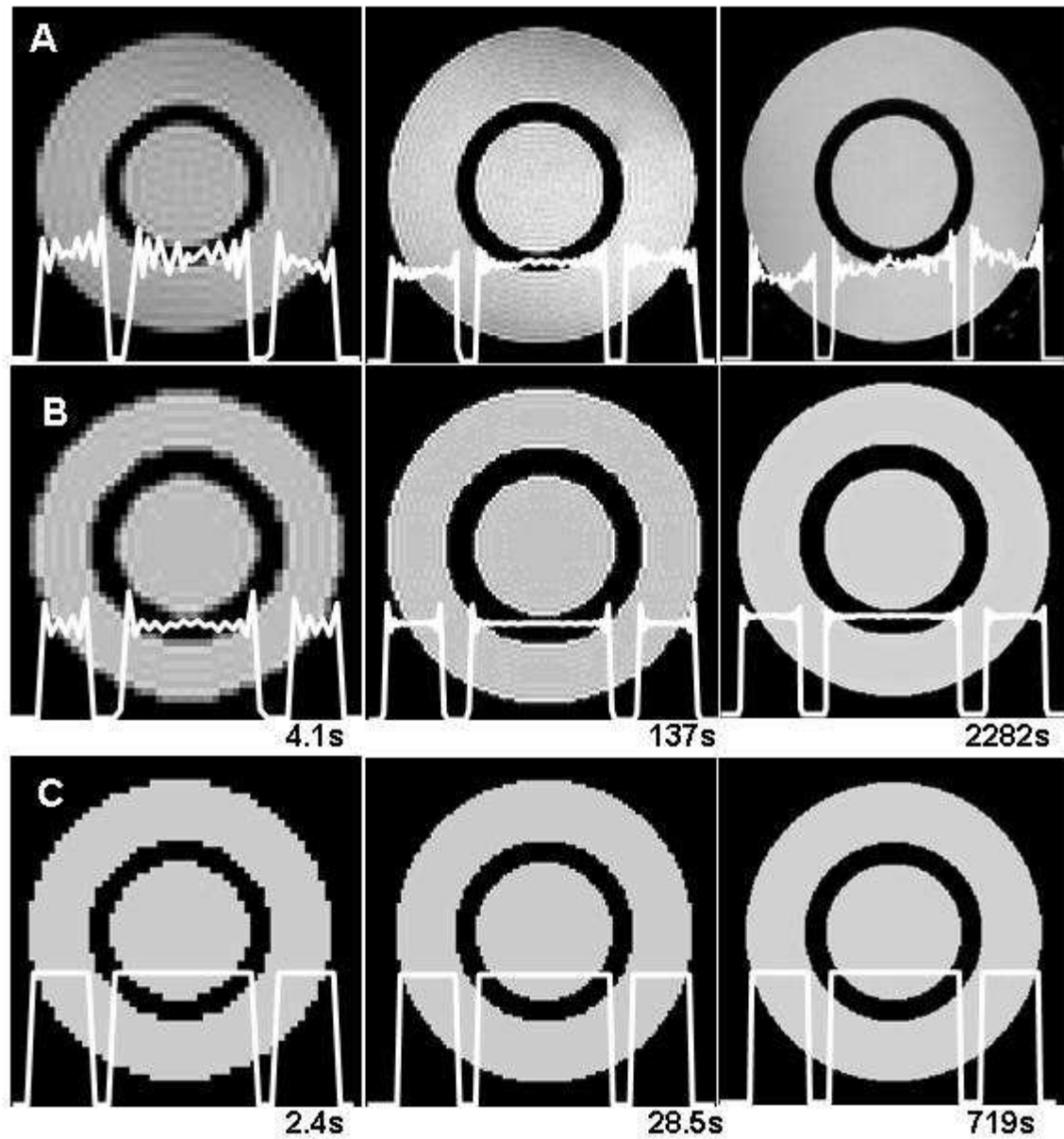
Fig.7. Comparison of Gibbs artifacts in real and simulated images using different spatial resolutions (sample model and image have identical matrix size): 64x64 left, 128x128 middle and 256x256 right columns. The top row shows images of a water-filled phantom acquired on 11.7T scanner. The middle and bottom row are simulated images with and without using IVD, respectively. Although images without dephasing are perfectly smooth, the images with IVD have a much closer resemblance to the experimental data. The time required for simulation is indicated at bottom of each simulated image.
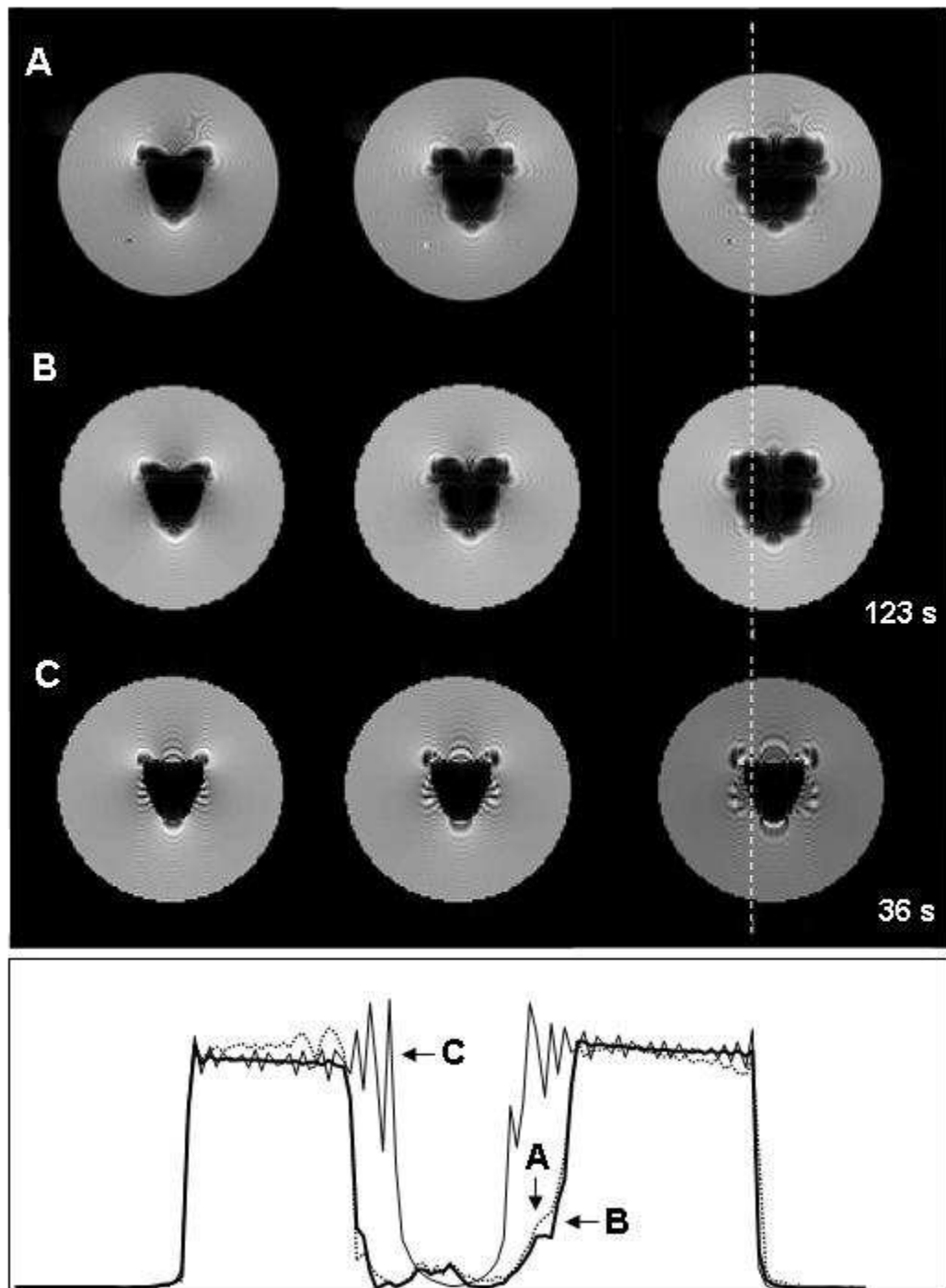
Fig.8. Comparison of experimental and simulated gradient echo images with various echo times of 10, 15 and 25 ms from a cylindrical phantom containing an axially placed air-filled tube: (A) row of experimental images from a 3 T scanner, (B) row of simulated images with IVD and (C) row of simulations without IVD. The profiles through the phantom center (location marked by a vertical white dotted line) for data sets with TE = 25 ms are shown as well at the bottom of the figure. The typical simulation times are indicated as well.